SANDIA REPORT

SAND97–0750 • UC–110
Unlimited Release
Printed April 1997

Fuel Cell Applications for Novel Metalloporphyrin Catalysts
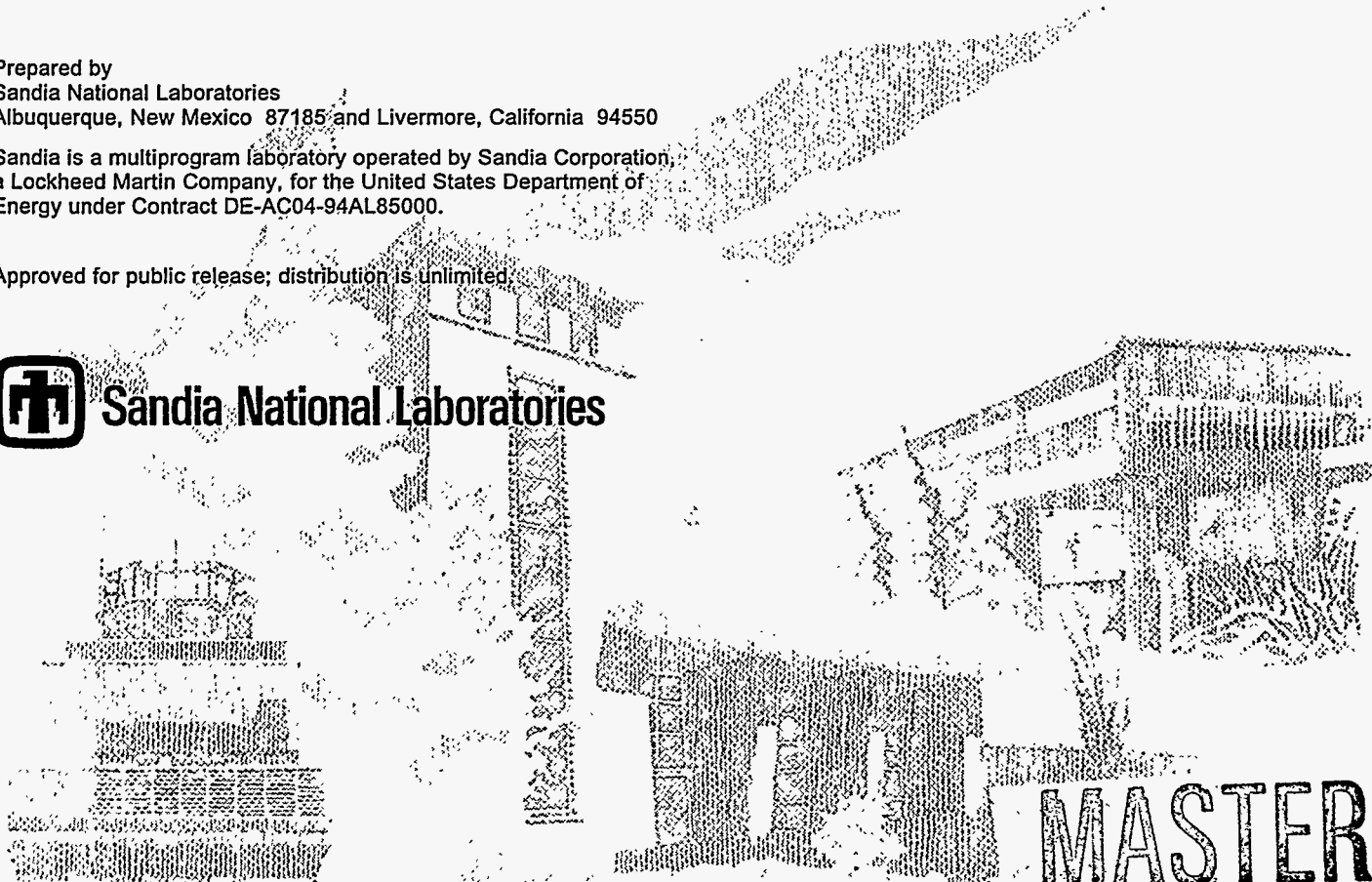
RECEIVED
MAY 0 5 1997
OSII

Gail Ryba, John Shelnutt, Narayan Doddapaneni, Kevin Zavadil

Approved for public release; distribution is unlimited.

Sandia National Laboratories

MASTER

DISTRIBUTION OF THIS DOCUMENT IS UNLIMITED

SF2900Q(8-81)

DISCLAIMER

Portions of this document may be illegible in electronic image products. Images are produced from the best available original document.

Fuel Cell Applications for Novel Metalloporphyrin Catalysts

Gail Ryba, John Shelnutt, Fuel Science Department
Narayan Doddapaneni, Exploratory Battery Department
Kevin Zavadil, Surface And Sensor-Controlled Processes Dept.
Sandia National Laboratories
P.O. Box 5800
Albuquerque, NM 87185-0710

ABSTRACT

This project utilized Computer-Aided Molecular Design (CAMD) to develop a new class of metalloporphyrin materials for use as catalysts for two fuel cell reactions. The first reaction is the reduction of oxygen at the fuel cell cathode, and this reaction was the main focus of the research. The second reaction we attempted to catalyze was the oxidation of methanol at the anode. Two classes of novel metalloporphyrins were developed. The first class comprised the dodecaphenylporphyrins whose steric bulk forces them into a non-planar geometry having a pocket where oxygen or methanol is more tightly bound to the porphyrin than it is in the case of planar porphyrins. Significant improvements in the catalytic reduction of oxygen by the dodecaphenyl porphyrins were measured in electrochemical cells. The dodecaphenylporphyrins were further modified by fluorinating the peripheral phenyl groups to varying degrees. The fluorination strongly affected their redox potential, but no effect on their catalytic activity towards oxygen was observed. The second class of porphyrin catalysts was a series of hydrogen-bonding porphyrins whose interaction with oxygen is enhanced. Enhancements in the interaction of oxygen with the porphyrins having hydrogen bonding groups were observed spectroscopically. Computer modeling was performed using Molecular Simulations' new CERIUS^2 Version 1.6 and a research version of POLYGRAF from Bill Goddard's research group at the California Institute of Technology. We re-optimized the force field because of an error that was in POLYGRAF and corrected a problem in treatment of the metal in early versions of the program. This improved force field was reported in a *J. Am. Chem. Soc.* manuscript. Experimental measurements made on the newly developed catalysts included the electrochemical testing in a fuel cell configuration and spectroscopic measurements (UV-Vis, Raman and XPS) to characterize the catalysts.

ACKNOWLEDGMENTS

We would like to acknowledge the assistance of several colleagues who were instrumental in the success of this project. Dr. Craig Medforth and graduate students in the laboratory of Dr. Kevin Smith, in the Chemistry Department of the University of California at Davis worked very hard to synthesize the complex new catalysts developed in this work. They also provided analysis of these materials, particularly the NMR characterization. Dr. J. Martin E. Quirke, in the Chemistry Department of Florida International University, synthesized the complex hydrogen-bonding porphyrins. Professor Jose Colucci, of the Chemical Engineering Department of the University of Puerto Rico-Mayagüez, introduced us to the use of gas-diffusion electrodes in electrochemical cells. Professor Colucci's students, Rosa Bures Berry, Vanessa Montalvo Rivera, and Pedro Diaz Pabon, took much of the data for this project during summers at Sandia National Laboratories.

TABLE OF CONTENTS

INTRODUCTION

The goal of this project was the development of a new class of metalloporphyrin materials as catalysts for use in fuel cell applications. Fuel cells have been identified as a critical technology for DOE's advanced transportation program. Both the President's National Critical Technologies Panel and the National Energy Strategy recognize the importance of this technology for transportation (as well as stationary power) applications. Fuel cells are being considered as alternative power sources for many applications, including large systems such as transportation and utility applications and small and micro systems where fuel cells may prove to be more valuable than batteries. Fuel cell powered vehicles would be energy efficient, potentially fuel flexible, and environmentally sound when compared with internal combustion vehicles. The H_2/O_2 fuel cell can theoretically achieve 98% efficient energy conversion (calculated using the Lower Heating Value of H_2), and realistically, 85%, when the byproduct heat is utilized. This efficiency, in and of itself, would result in significant reduction in both fuel consumption and environmental pollution; proposed sources for renewable hydrogen make fuel cell use even more environmentally benign. Moreover, because hydrogen is the one of the highest density energy carriers available, a fuel cell is potentially the highest energy density device available for powering any need. It has been estimated that H_2/O_2 fuel cells can achieve energy densities of 1000 Wh/kg, while Li/polymer batteries have energies densities of about 400 Wh/kg.[1] In the short term, however, the low temperature fuel cells, such as the polymer electrolyte fuel cell (PEFC), will have to run on hydrogen produced by reforming fuels, or directly through the electrooxidation of fuels such as methanol and methane. To make either fuel source economically practicable, a number of materials issues must be solved.

Fuel cells are essentially refuelable batteries in which a fuel (generally hydrogen or methanol for transportation applications) is converted directly into electricity without an intermediate combustion process. The fuel is oxidized at a catalytically active anode while an oxidant (air) is reduced at a catalytically active cathode. Current then flows through the external load with an ionic electrolyte between the electrodes providing charge balance. The key processes which determine a fuel cell's efficiency and reliability are the catalytic interactions at the electrodes. At present, platinum and/or ruthenium are used as the catalyst at both electrodes. Platinum impregnated electrodes, however, have

several operational drawbacks: 1) they are unstable under long-term use; 2) they are poisoned by small amounts of impurities such as CO; and 3) they are expensive and of limited availability. It was recognized in the workshop on "Basic Research Needs for Vehicles of the Future"[2] that the development of stable, efficient, poisoning-resistant, inexpensive, non-noble metal catalysts would represent a major breakthrough in fuel cell technology.

At a more fundamental level, the reactions of interest in fuel cell electrochemistry are inherently complex and their catalysis, even at platinum, is not well understood. When used for the oxygen cathode reaction, catalysts must perform either a four-electron reduction of oxygen to water, (or a two-electron reduction to peroxide, followed by a very rapid two-electron reduction to water) and should be chemically and electrochemically inert towards anode fuels such as hydrogen and methanol. New catalysts for the anode reaction must be resistant to CO and sulfur poisoning, both when hydrogen from reformate is used and in direct methanol oxidation. For direct methanol fuel cells, catalysts must catalyze the 6-electron oxidation of methanol to carbon dioxide.

Problems being encountered with present catalytic materials include: low catalytic activity, poor stability in fuel cell working environments, mismatch of redox potentials with the appropriate chemical reactions, susceptibility of catalysts to poisoning from impurities, availability and cost. The catalyst design also sought to inhibit the aggregation of catalyst molecules into clusters which reduces catalytic activity, and we sought ways to attach the catalyst molecules to a carbon substrate electrode to make the catalysts useful in fuel cells. Proper design of these materials could provide solutions to many (and potentially all) of the present limitations, particularly for the fuel cell systems that are most appropriate for transportation applications (PAFC, AFC, and PEM fuel cells).

In particular, we pursued the following:

1) To reduce the susceptibility of the catalyst to poisoning effects, we varied the central metal atom and side chain groups of a metalloporphyrin to make it more or less reactive towards other molecules. The steric and electronic properties of the dodeca-substituted metalloporphyrins can be varied to a degree not possible with a pure noble metal, or even other less-substituted macrocyclic molecules.

2) To inhibit aggregation of the catalyst molecules, we designed molecules with side groups that lead to non-planar geometries. The planar geometry of presently-used macrocyclics allows the molecules to stack on top of each other which blocks diffusion to and interaction with the active sites. The ruffled geometry of the substituted metalloporphyrins inhibits aggregation while allowing other desirable characteristics to be built in (e.g. - proper molecular spacing, chemical stability, proper pocket size formation).

3) Previous work has shown that 2-electron processes can occur when O_2 has access to both sides of a macrocyclic catalyst. We designed porphyrins in which one side of the molecule is blocked by appropriate side chains, increasing the 4-electron reduction process relative to 2-electron processes.

4) The new class of porphyrins we proposed to use allows the redox potential of the molecules to be varied over a much larger (factor of 5) range than for conventional porphyrins. This is done by varying the electron withdrawing properties of the substituted side-groups. Increasing the electron affinity of side-groups can also be used to increase the stability of the metalloporphyrin in an acidic or basic solution.

5) These catalysts are also good candidates as direct methanol oxidizers (under certain conditions metalloporphyrins have been shown to have 10 times the catalytic activity of platinum in this regard). Stability of the central metal atom in solution has been the principal problem here and (as discussed in point 4 above) we attempted to solve this problem with proper molecular design. There would be an application for this technology in fuel reformers as well (a pre-stage to the fuel cell that turns a fuel, such as methanol, into hydrogen).

This technology is particularly well suited to the low operating temperatures and chemical environments of the fuel cell systems that are most appropriate for transportation applications.

BACKGROUND

At low temperature (80°C) the cells utilizing Pt and Ru lose as much as 30% or their potential output due to losses caused by the poor catalysis of the oxygen reduction reaction. We chose to study porphyrins because they comprise the active sites of biological enzymes, such as cytochrome c oxidase which are effective catalysts for oxygen reduction. An important goal of the work reported here was our

intent to develop more sophisticated systems which more closely mimic biological systems while still retaining sufficient simplicity to be viable in a man-made device, such as a fuel cell.

It was recognized in 1964 that transition metal macrocycles are able to reduce oxygen and might be viable catalysts in fuel cells.[3] Over the succeeding years, workers evaluated the most common porphyrins and phthalocyanines, including complexes of iron, cobalt, nickel, copper, magnesium, vanadium, chromium and hydrogen, and the most common ligands, including tetraphenylporphyrinato, octaethylporphyrinato, tetrasulfonatedporphyrinato, tetrasulphonatedphthalocyaninato (TSPc), tetramethoxyphthalocyaninato, octamethoxyphthalocyaninato, tetraneopentoxyphthalocyaninato, naphthalocyaninato (Npc),[4] tetrakis(N-methylpyridinium-4-yl)porphyrinato[5] and others. Most previous macrocycle work has focused on relatively simple, planar porphyrin and phthalocyanine systems. The major exception to this statement is represented by the work of Collman[6] and Anson[7] who have utilized novel and sophisticated cofacial geometries, or multiple metal centers attached to their porphryins to enhance four-electron reduction over two-electron reduction of dioxygen. In spite of this, none of these compounds has replaced Pt in commercial devices, although a cobalt tetramethoxyphenyl porphyrin electrode is commercially available for research,[8] and there are scattered reports of stable systems, particularly in alkaline electrolytes. More recently, pyrolysis of the N_4-chelates has shown promise for generating stable catalysts, but the changes leading to improvement have not been fully identified, and the optimal temperature appears to vary.[9] Recent work in the Exploratory Battery Department at Sandia has shown an optimal temperature of 350 C, and they have preliminary evidence of catalyst polymerization, which others have also suggested.[10] This work has also demonstrated the need for a better fundamental understanding of the physical and chemical processes involved.

RESULTS

The synthesis, computer modeling, electrochemical data and spectroscopic studies for this work are presented in this report.

Catalyst Synthesis:

Synthesis of the iron and cobalt derivatives of the fluorinated dodecaphenylporphyrins (DPP) in the laboratories of Kevin Smith at the University of California at Davis was successful and yielded quantities suitable for catalyst testing. This required the scaled-up re-synthesis of the entire series. The compounds are: CoDPP, $CoDPPF_8$, $CoDPPF_{20}$, and $CoDPPF_{28}$. These halogenated porphyrins are of interest because of (1) their high stability, (2) the presence of an O_2-binding cavity, and (3) their novel electronic properties, which will extend the range of redox potentials for this series in the negative direction. Figure 1 shows the iron analogs of the dodecaphenyl systems that were evaluated in this study. Efforts are still underway to synthesize more highly fluorinated versions of CoDPP via the Susuki reaction (see Figure 2)

Fe(III)Dodecaphenylporphyrin

Fe(III)DodecaphenylporphyrinF$_{20}$ (FeDPPF$_{20}$)

Fe(III)DodecaphenylporphyrinF$_{28}$ (FeDPPF$_{28}$)

Figure 1 Dodecaphenyl porphyrins

Susuki Reaction

Co(II)TPPBr$_8$

$$R = \begin{array}{c} R_3 \cdots C \cdots R_1 \\ | \\ R_2 \end{array}$$

Co(II)TPP chiral derivative
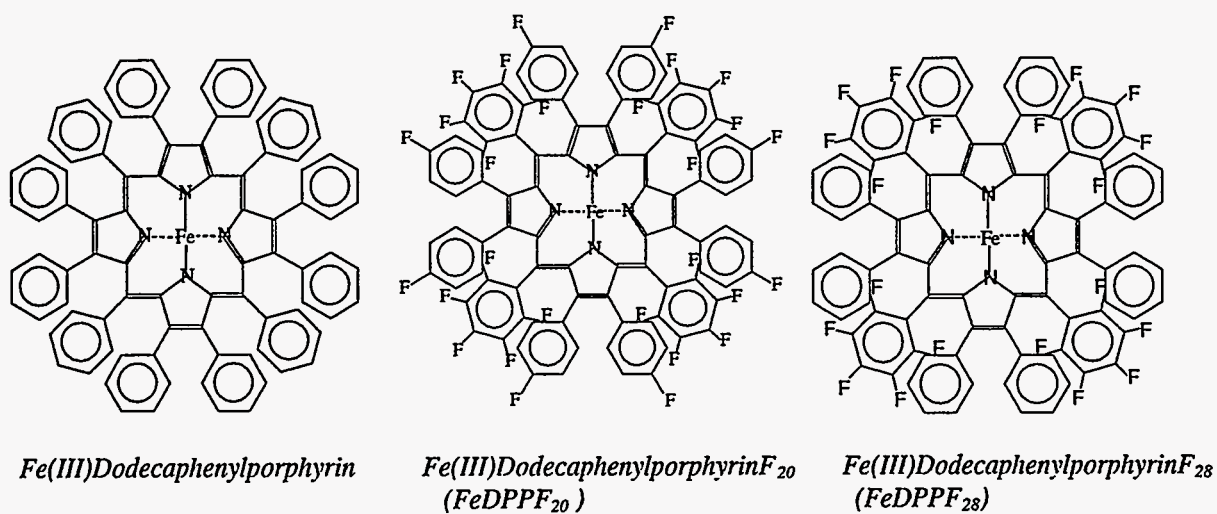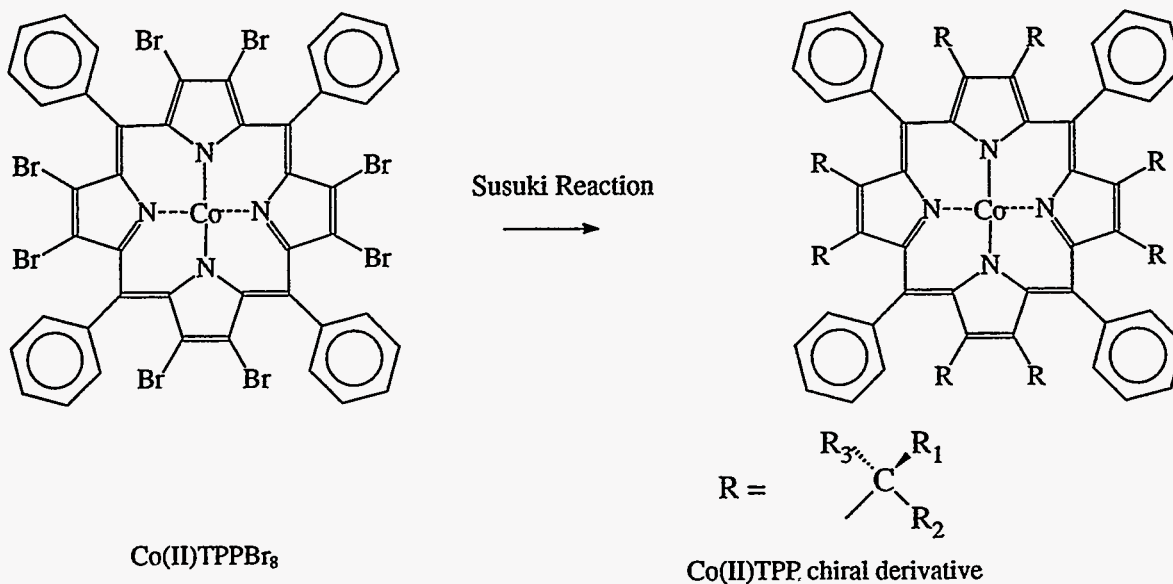
Figure 2 The synthesis of cobalt derivatives of tetraphenylporphyrins with chiral pyrrole substituents.

In addition to the creation of a "pocket" to enhance the interactions of the catalyst with the oxygen, the sterics of these new molecules also prevent aggregation, and enable access to the catalytic site.

Computer Modeling:

Molecular mechanics calculations were performed on two of our initial designed catalyst candidates, Cobalt dodecaphenyl porphyrins (CoDPP) and on two of its fluorinated derivatives (CoF20DPP and CoF28DPP). These calculations showed that these molecules should both take on similar ruffled conformations. This geometry provides a binding pocket for the reactant (O_2) (see Figure 3) and may also help prevent aggregation of the molecules which could lead to active site obstruction. To test whether or not this second assertion is reasonable (that a ruffled geometry can prevent active-site blocking), molecular dynamics calculations of planar and ruffled porphyrins were performed. These calculations showed that planar porphyrins do indeed have a strong tendency to stack (Figure 4). This planar stacking completely blocks interior active site access, effectively limiting the amount of catalyst that can be attached to a substrate. On the other hand, molecular dynamics calculations on ruffled porphyrins show that a fairly ordered yet open structure is formed. This open structure should increase access to the active sites, which should allow a higher concentration of these materials to be attached to an electrode, increasing the overall catalytic activity. (Figure 5).
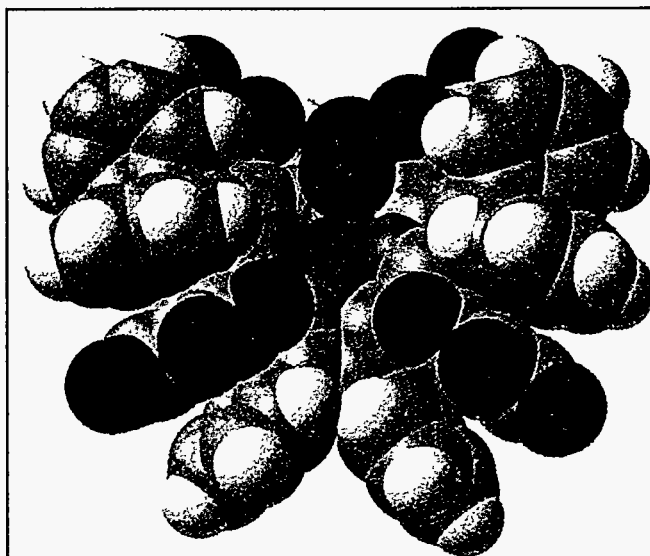

Figure 3 Oxygen in the binding pocket of a cobalt dodeca-substituted porphyrin catalyst with electron-withdrawing perfluorophenyl side groups designed to enhance catalytic activity by modifying redox potentials, decreasing aggregation, and increasing central metal atom stability.
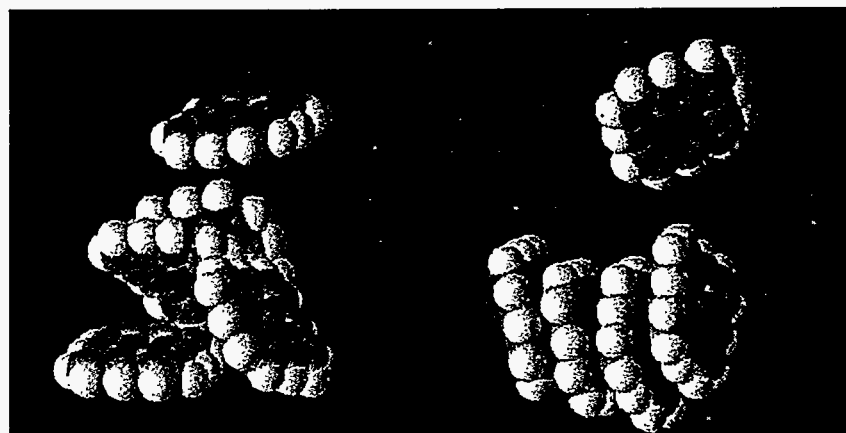
Figure 4. Molecular dynamics simulation of planar porphyrins. Initial configuration (left) and configuration after 10 ps (right). Note the strong tendency for stacking and the obstruction of the active sites.
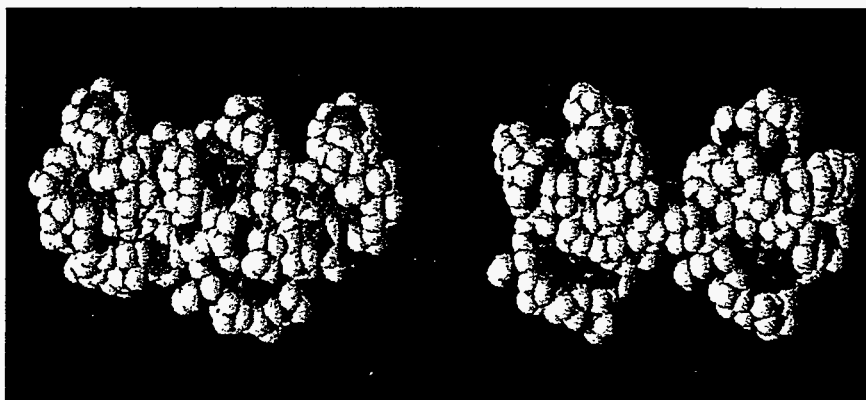
Figure 5. Molecular dynamics simulation of ruffled porphyrins. Initial configuration (left) and configuration after 20 ps (right). Note the ordered yet open final configuration and accessibility of the active sites.

In the last year of this project, we studied a series of non-planar porphyrins having differing numbers of fluorine substituents on the porphyrin ligand and spanning a 400 mV range in redox potential. Our results suggested that we needed to increase the interactions between the oxygen and catalyst, so we

Figure 6a Oxygen (red bar above molecule) minimizes off-center from the cobalt atom in 5,15 bis(hydroxymethyl) octaethylcobalt porphyrin

Figure 6b. Oxygen (red bar above molecule) minimizes in the center above the cobalt in 5,15-dichloro-10,20 bis(hydroxymethyl) octaethylcobalt porphyrin.

Figure 7 Top View: O₂ above 5,15-dichloro-10,20-bis(hydroxymethyl) Co Octaethylporphyrin

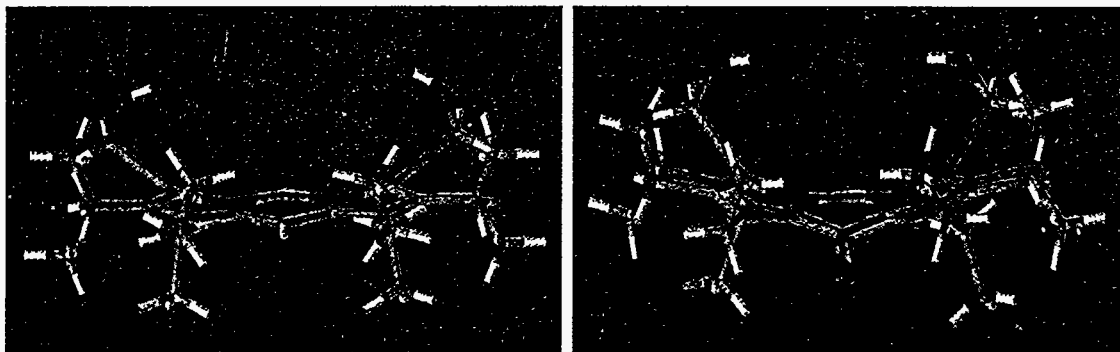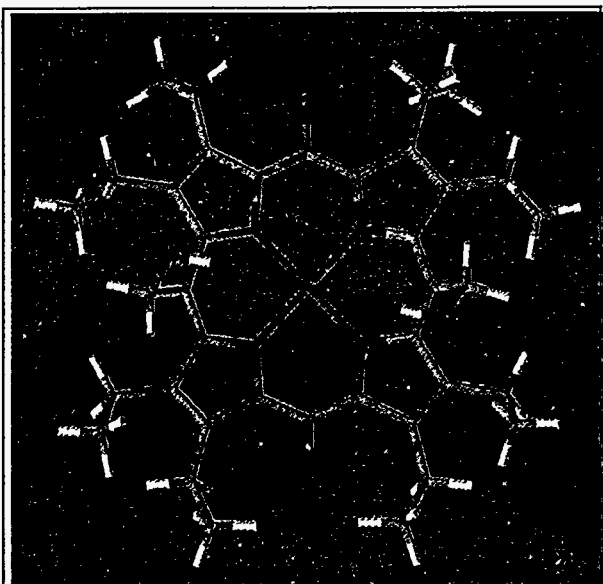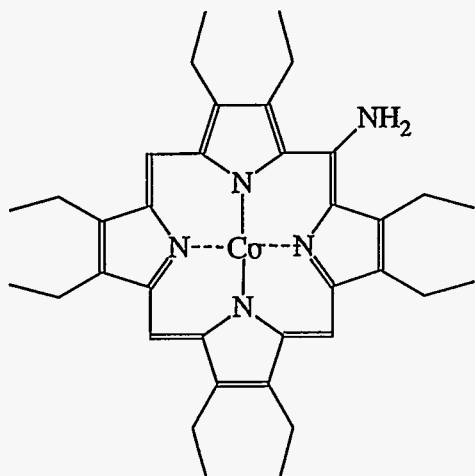used computer modeling to design a third generation series of catalysts with hydroxy, formyl and amino functional groups that would have hydrogen-bonding interactions with the oxygen. Figure 6 shows a porphyrin with two hydroxymethyl groups, one on each side of the porphyrin, on the 5 and 15 positions. In Figure 6a, there are hydrogens at the 10 and 20 positions, and the energy minimized structures suggests that the oxygen molecule will interact with one of the hydroxymethyl groups more strongly than the other, leading it to an energy-minimized off-center location. In Figure 6b, the 10 and 20 positions are substituted with the larger chlorine atom, and steric interactions force the hydroxymethyl groups further in toward the center of the molecule. This porphryin is shown from the top in Figure 7. This slight change in the porphyrin pocket causes the oxygen to interact equally with the hydroxymethyl groups, and causes it to line up directly over the center of the molecule which we expect optimizes the potential for catalysis. We are awaiting the synthesis of sufficient quantities of catalysts in this family for fuel cell testing. Very small amounts of catalysts with half the desired hydrogen-bonding features (shown in Figure 8) were synthesized, and Raman measurements indicate that interactions between the functional groups and small molecules containing H-bond acceptors do occur. These results are discussed in the section on spectroscopy results below.

Figure 8 Cobalt 5-amino-octaethyl-porphyrin. The amino group is an H-bond donor and acceptor.

Porphyrin/O$_2$ Complex	E(porphyrin/O$_2$ Complex)	((E(porphyrin) + E(O$_2$))	ΔE	E(H-bonds)
Energies in kcals/mole				
CoOEP	148.8	152.9	-4.1	0.0
Co(5-NH$_2$)OEP	161.3	177.4	-16.1	-13.2
Co(5-CH$_2$OH)OEP	172.8	191.3	-18.5	-13.7
Co(5,15-CH$_2$OH)OEP	204.9	222.2	-17.3	-13.7
Co(5,15-CH$_2$OH- 10,20-Cl)OEP	251.9	273.8	-21.9	-17.5

Table 1 Calculated Binding Energies For O$_2$. Our 3rd generation of catalysts incorporates hydrogen bonding groups. The energies associated with a series of the cobalt octaethylporphyrins are tabulated above (the last two are shown in Figure 6). The column under ΔE indicates the extent to which the complex energy is lowered over that of the separated pairs.

Development of New Modeling Methods. We have been using Molecular Simulations' new CERIUS^2 Version 1.6 and Bill Goddard's research version of POLYGRAF, which we obtained while on a working visit to CalTech. The latter program has quite a bit of functionality that is not in the commercial version and allow us to accurately predict not only the conformation of the molecules but also the energies and vibrational spectra of the various conformers (local minima). We completed the computer-optimization of the molecular mechanics force field to the experimental data, and we also re-optimized the force field because of a minor error that has been in POLYGRAF from the beginning. This new force field corrects a minor problem in treatment of the metal in earlier versions and uses a periodic cosine function for the angle term of the metal. This improved force field was used in the calculations reported in a *J. Am. Chem. Soc.* manuscript.

Electrochemical Testing:

Both glassy carbon and carbon gas diffusion electrodes were used to examine the catalysts. To prepare glassy carbon electrodes (Bioanalytical Systems, Inc., West Lafayette, Indiana, 3.0 mm diameter, Part no. MF-2070), the electrodes were coated with a solution of the porphyrin, and the solvent was allowed to evaporate leaving a film of the desired porphyrin on the surface.
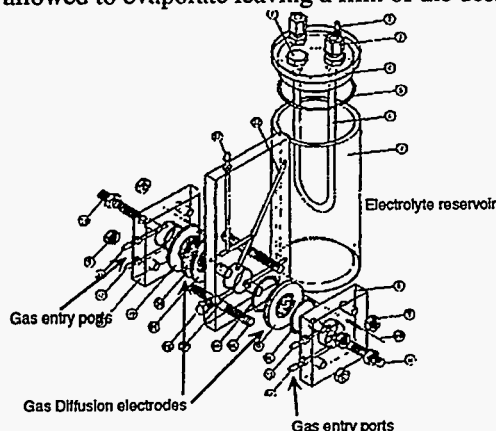

Figure 9 Schematic of ASTRIS Quickcell, taken from product literature. Astris, Inc., 2480 Dunwin Dr., Mississauga, Ontario, Canada L5L 1J9

When using gas diffusion electrodes, a modified ASTRIS Quickcell was used. This cell is shown in Figure 9. The O$_2$ electrode consisted of an Alupower [Electrosynthesis Corp., Lancaster, NY] gas diffusion electrode modified with the Co-porphyrin catalyst. The Co-porphyrin catalyst was added by soaking the gas diffusion electrode in a pyridine or CS$_2$ solution of the catalyst. No significant difference is observed for electrodes prepared from pyridine and CS$_2$.

The cell was also been modified so that a smaller area electrode could be utilized. This meant that smaller amounts of the porphyrin catalyst could be tested. This was important since much smaller expenditures in resources is required and environmental, health, and safety concerns were reduced. In our standard catalyst test, 0.68 μmoles of catalyst were loaded onto the 5-cm^2 electrodes, providing roughly 0.14 μmole of catalyst/cm^2, or 8 μg of cobalt/cm^2. The effects of solvent, rates of drying, and catalyst loadings were evaluated.

Metalloporphyrins [Co(II)DPP, Co(II)F$_{20}$DPP, Co(II)F$_{28}$DPP and Ni(II)DPP] used in these experiments were provided by Dr. Craig Medforth at the University of California at Davis. Tetrabutylammonium tetrafluoroborate, lithium perchlorate, anhydrous dichloromethane and anhydrous dimethylsulfoxide were purchased from Aldrich.

1 mM metalloporphyrin solutions were prepared in 5mL solvent (CH$_2$Cl$_2$ or DMSO) using 0.1M tetrabutylammonium tetrafluoroborate (TBATFB or LiClO$_4$) as an electrolyte. A cyclic voltammogram (CV) of the blank (0.1M TBATFB in CH$_2$Cl$_2$) or (0.1M LiClO$_4$ in DMSO) were taken using glassy carbon as a working electrode, Pt wire as a counter electrode and a Ag wire (or Ag/AgNO$_3$ in the same solvent) as a reference electrode before investigating the redox properties of the metalloporphyrins. All CVs were taken using a Pine Instruments bipotentiostat model AFCBP1 under argon. Argon was purged for at least twenty minutes before any CVs were taken.

Metalloporphyrins for polymerization, the cobalt (II)-Tetra (2-aminophenyl)porphyrin [Co(II)T(2-NH$_2\phi$)P] used in these experiments were purchased from Midcentury Chemicals, Posen, Illinois. These porphyrins are insoluble in water but soluble in organic solvents such as CH$_2$Cl$_2$, CH$_3$CN and DMSO. Tetrabutylammonium tetrafluoroborate (TBATFB), lithium perchlorate (LiClO$_4$) anhydrous acetonitrile and anhydrous aniline were purchased from Aldrich.

In the electropolymerization experiments 10 mM (or 0.1M) monomer solutions were prepared in 10mL solvent (CH$_2$Cl$_2$ or CH$_3$CN) using 0.1M tetrabutylammonium tetrafluoroborate (TBATFB) as an electrolyte. The cell conditions were the same as reported for the CV measurements above. Aniline was polymerized by scanning between -0.50V and + 1.60 V five to ten times at 50 mV/s.

Measurement of redox potentials

Electrochemical characterization shows that the measured redox potentials follow the trends indicated by the summation of the Hammett constants for the porphyrin substituents. Raman spectroscopy - through the measurement of shifts in structurally sensitive frequency markers - also correlates well with both the structures calculated through molecular modeling as well as with the measured changes in the redox potential. The tunability range for the redox potentials is extended by over 0.5 eV beyond that of conventional porphyrin materials.

CVs of the dodecaphenyl porphyrins were measured in many solvents. Data for methylene chloride and dimethylsulfoxide are shown in Figure 10 and Figure 11, and the corresponding peak positions are recorded in Table 2 and Table 3, respectively. As expected, the peak positions shift positive with increasing numbers of fluorine atoms on the porphyrin. Relative shifts for peaks believed to correspond to the same type of redox processes are tabulated in the right-most column.

Anodic peak (V)	Cathodic peak (V)	E$_{1/2}$ (V)	
	Compound: Co(II)DPP File name: Codp018.dat		
-1.03	-1.19	-1.11	-
-0.508	-0.634	-0.57	-
0.989	0.820	0.91	-
1.20	1.01	1.11	-
	Compound: Co(II)F$_{20}$DPP File name: 2cf2010.dat		
			ΔE relative to non-fluorinated DPP
-1.34	-1.46	-1.4	
-0.194	-0.311	-0.25	0.32
1.57	1.41	1.49	0.58
1.68	1.59	1.64	0.53
	Compound: Co(II)F$_{28}$DPP File name: 2cf2810.dat		

			ΔE relative to CoF$_{20}$DPP
-1.29	-1.43	-1.36	0.04
-0.0696	-0.026	-0.17	0.08
1.63	1.47	1.55	0.06
1.81	1.67	1.74	0.10

Table 2 Half-Wave Potentials [E$_{1/2}$ in volts versus Ag wire] for reduction and oxidation of Co(II) and Ni(II)DPP Series in CH$_2$Cl$_2$ containing 0.1M TBATFB

Anodic (V)	Cathodic (V)	E$_{1/2}$ (V)	
	Compound: Co(II)DPP File name: Codpp3.dat		
-2.068	-2.144	-2.11	
-0.939	-1.028	-0.984	
0.005	-0.276	-------	
0.464	0.642	0.67	
0.699	------	-------	

	Compound: Co(II)F$_{20}$DPP File name: Cof20dp7.dat		
			ΔE relative to non-fluorinated DPP
-1.65	-2.36	-1.69	0.420
-0.629	-1.73	-0.76	0.224
0.315	-0.895	0.103	
--------	-0.109	-------	
	Compound: Co(II)F$_{28}$DPP File name: Cof28dp4.dat		
			ΔE relative to CoF$_{20}$DPP
-1.54	-1.67	-1.6	0.09
-0.555	-0.884	-0.72	0.04
---------	-2.35	-------	

Table 3 Half-Wave Potentials [E$_{1/2}$ in volts versus Ag/AgNO$_3$] for reduction and oxidation of Co(II) DPP series in DMSO containing 0.1M LiClO$_4$

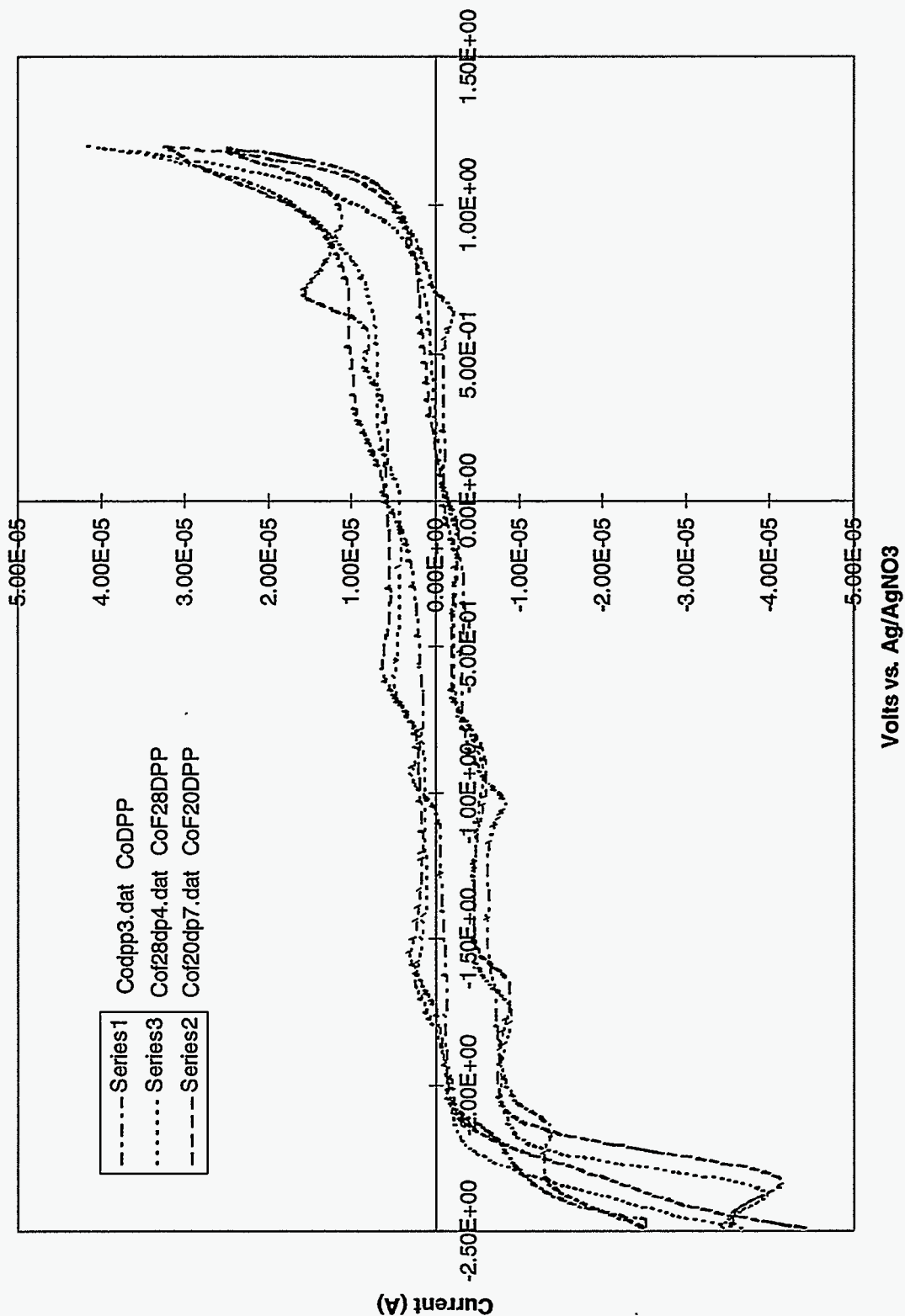## Co(II) DPP Series/0.1M LiClO$_4$/DMSO

Figure 10 Cyclic voltammograms for fluorinated cobalt dodecaphenylporphyrins in dimethylsulfoxide.
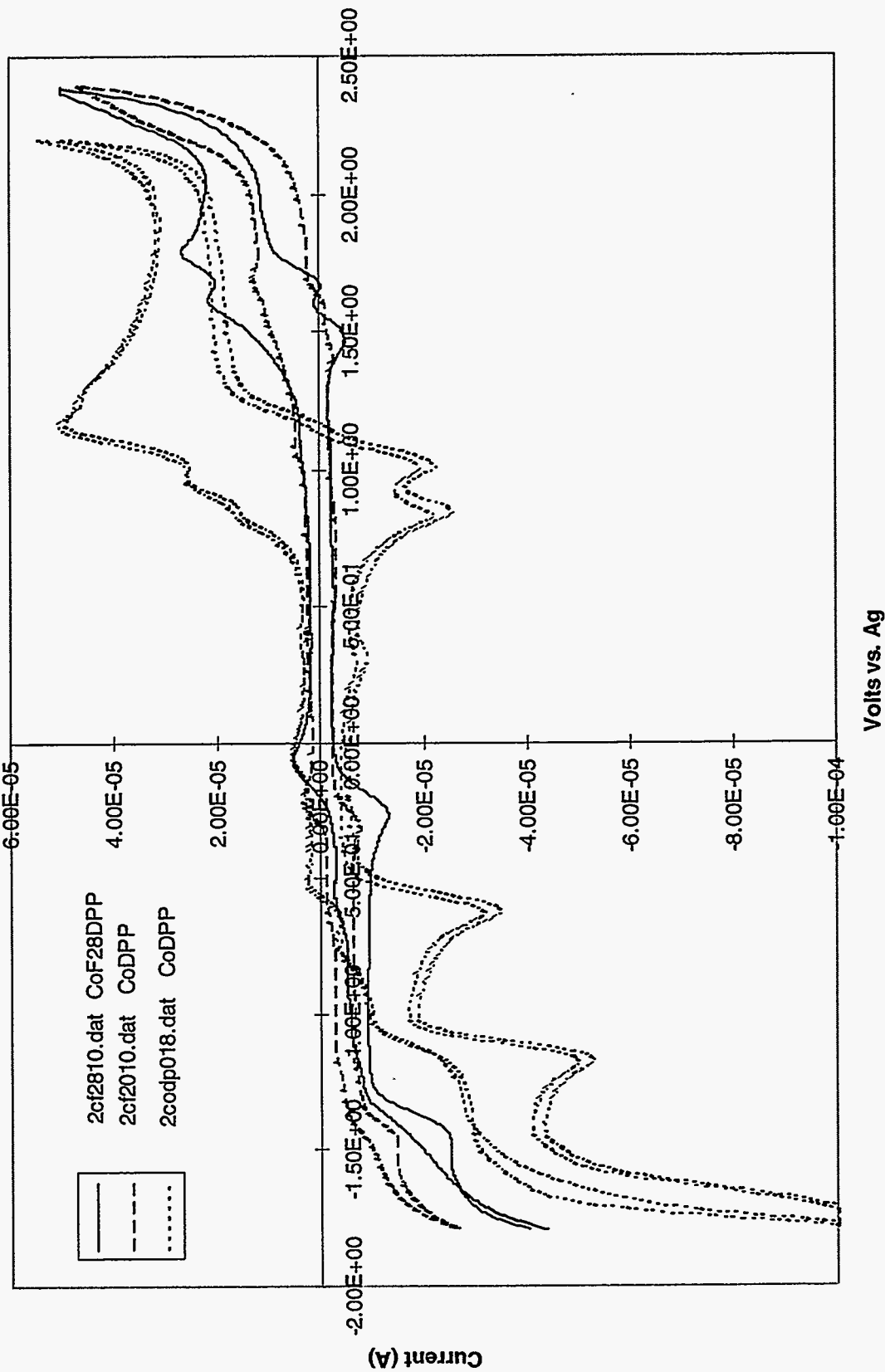
Co(II)DPP Series/CH₂Cl₂/TBATFB

Figure 11 Cyclic voltammograms for fluorinated cobalt dodecaphenylporphryins in methylene chlorine.

Reduction of oxygen using the new catalysts

When using glassy carbon electrodes coated with porphyrins, we observed a reduction in the overpotential for oxygen reduction. Potentials measured in these experiments are tabulated in Table 4.

	E_0 vs NHE (mV) Catalyst prepared from pyridine	E_0 relative to blank (mV) Catalyst prepared from pyridine	E_0 relative to blank (mV) Catalyst prepared from CH_2Cl_2
Blank	-240	0	0
Pyridine	-220	+20	--
Planar			
CoOEP	-170	+70	0
CoTPP	-170	+70	--
Non Planar			
CoOETPP	-350	-110	+20
CoDPP	-300	-60	--
CoF$_{20}$DPP		+20-50	--

Table 4 Potentials for the reduction of O_2 in 1 M KOH, using porphyrin adsorbed to glassy carbon. A positive value relative to the blank means the reduction is catalyzed. OEP ≡ Octaethylporphyrin; TPP ≡ Tetraphenylporphyrin; OETPP ≡ Octaethyltetraphenylporphyrin; DPP ≡ Dodecaphenylporphyrin

Cyclic voltammagrams of these materials using glassy carbon electrodes show broad reduction waves rather than sharp peaks, which may be indicative of poor attachment or multiple attachment sites to the glassy carbon electrode substrates. This result led us to develop the use of gas-diffusion electrodes for further testing.

For use in an actual fuel cell the catalysts were loaded onto blank graphite-based, porous gas-diffusion electrodes. The catalysts performed very well in 1 M KOH, but of more import was the fact that a number of the catalysts performed well in 2 M sulfuric acid, where macrocyclic catalysts are traditionally less stable. A polarization curve taken for a cobalt porphyrin in 2 M sulfuric acid is shown in Figure 12. It can be seen that its performance compares favorably with that of platinum.

The improvement noted for gas-diffusion electrodes points to the importance of the electrode support. Most of the catalysts continued to be loaded on electrodes by adsorbing them from organic solvents. Electrodes were prepared using different solvents, rates of drying, weight loadings and treatment times to try and elucidate the effect of solvent and to effect enhanced coverages of the blank commercial gas diffusion electrodes. All of the methods tried resulted in roughly equal performance, and compared favorably with a commercially prepared cobalt porphyrin electrode, indicating that our low weight loadings are an effective way to measure the catalyst activity.

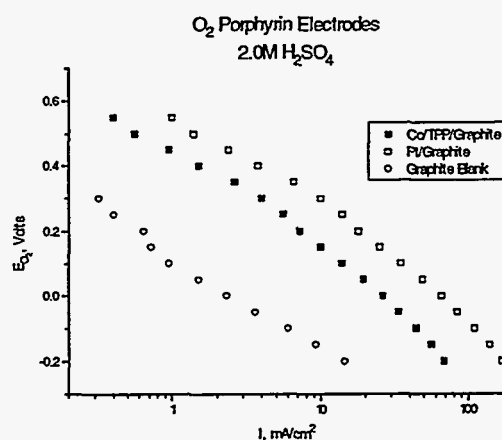Further work was performed on obtaining covalent attachment of the catalysts

Figure 12 Polarization curve of cobalt tetraphenyl porphyrin in 2 M sulfuric acid

to the carbon supports by derivatizing the carbon surface with an amino-pyridine which is expected to be an axial ligand for cobalt porphyrins. XPS studies of two different solid carbon supports (highly-ordered pyrolytic graphite (HOPG) and glassy carbon (GC)) were made between the three steps involved in making this linkage (anodization, amidization and porphyrin attachment). The HOPG surface shows the greater response to anodization with a larger net increase in surface oxygen and an oxidized form of carbon clearly visible in the C(1s) spectra. Both surfaces show significant affinity for amino-pyridine. The HOPG surface was the only sample that yielded a Co signal after catalyst loading. The detected cobalt on the HOPG surface was in a low spin configuration, suggestive of adsorptive attachment as opposed to fifth ligand attachment via the amine functionality. This suggests that the treatment may only be effective on some forms of carbons, and not necessarily on those being used in the commercial gas diffusion electrodes.

Data showing the performance of the dodecaphenyl porphyrins is all summarized in Figure 13. All three of the dodecaphenylporphyrins yielded higher voltages than the planar cobalt octaethylporphyrin and cobalt tetraphenyl porphyrin. They performed significantly better than the blank gas diffusion electrodes did, although not as well as commercially prepared platinum electrodes. However, the loading and wetting properties of these commercial electrodes are much more optimal than those of our laboratory coated porphyrin electrodes. These newly computer-designed catalysts with "grooves" reduce the overpotential of oxygen reduction by 50 mV at 10 mA/cm^2 relative to the planar porphyrins.

Data showing the performance difference in acid solutions relative to base solutions are shown in Figure 14. The axes have been adjusted by 59 mV/pH unit in order to compare the curves directly. Much higher voltages were obtained for electrodes in KOH cells, as has been found by others.

Finally, the stability of some of the planar cobalt tetraphenyl porphyrins was measured in acid solution. The decay in current for an oxygen cathode held at 0.4 V vs. Ag/AgCl is shown in Figure 15. Marked decays in the magnitude of the current are observed for both the blank electrode and the porphyrin treated electrodes. We sought to stabilize the catalysts and electrodes in the 80°C sulfuric acid electrolyte, but have not yet successfully done so. UV-Vis measurements were made of the electrolyte solutions after one and two hour tests in which the oxygen cathode potential was maintained at 0.4 V, but no porphyrin or porphyrin degradation products were observed in the electrolyte after the test.

In an attempt to stabilize the porphyrins on the solution of carbon electrodes, tetra-2-aminophenyl, tetra 4-aminophenyl, tetra 2-hydroxyphenyl and tetra-4-hydroxyphenyl porphyrins were polymerized onto the surface of carbon electrodes either in a pure form, or as copolymers with aniline or pyrrole. Films could be grown by holding the potential of the working electrode sufficiently positive to induce anodic polymerization, or by cycling the potential across a sufficiently wide potential window. The most robust films were grown using cobalt(II) meso-tetra 2-aminophenyl porphyrin with aniline. However, on glassy carbon electrodes, the polymer films peeled off before adequate testing for oxygen reduction could be performed. UV-Vis spectra of these films grown on indium tin oxide electrodes were also measured.
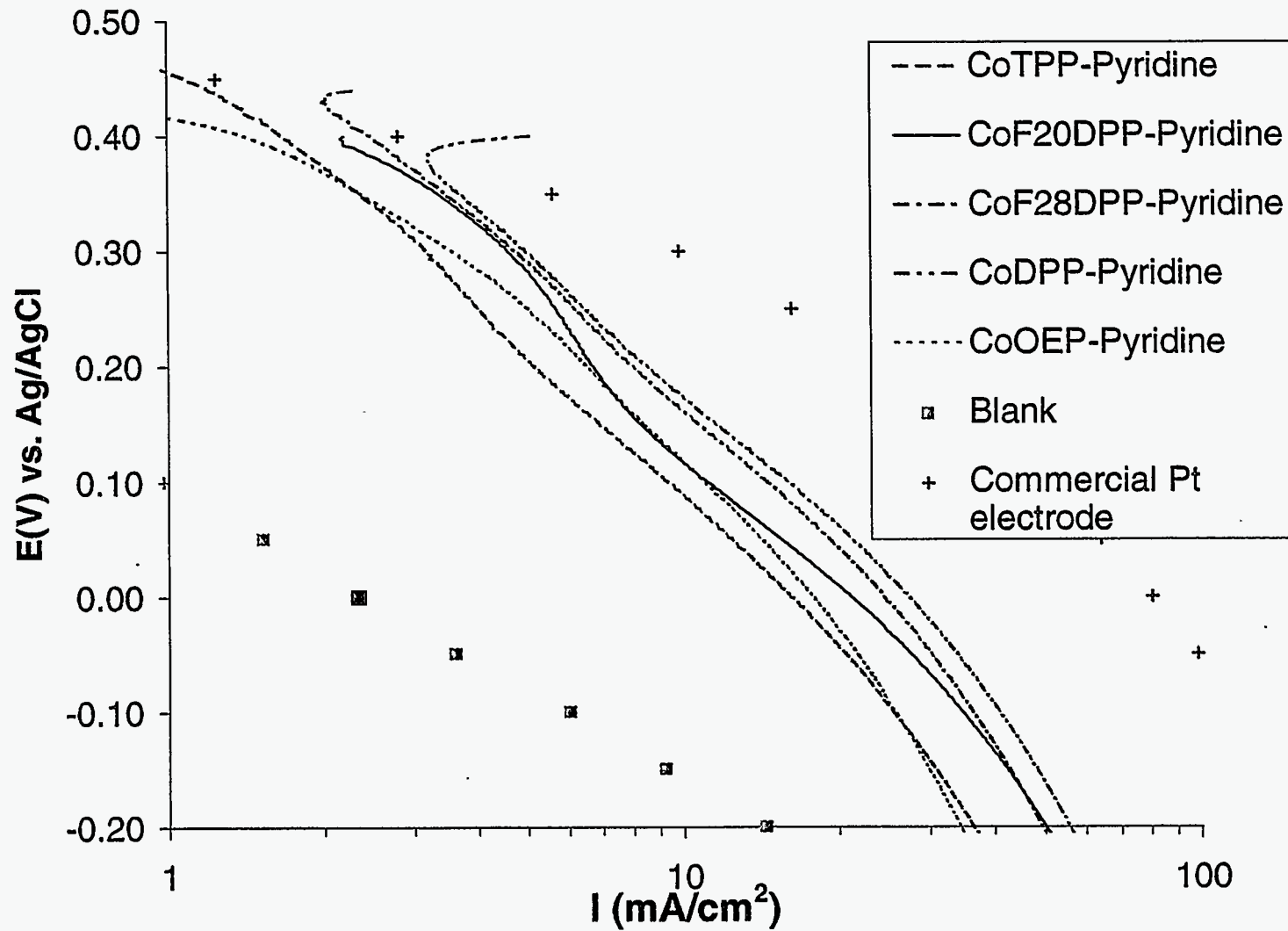
Figure 13 Summary slide of reduction of oxygen using cobalt dodecaphenyl porphyrins.

O$_2$ Reduction in Acid and Base
Using Co Dodecaphenyl Porphyrins
right y-axis is offset 840 mV for pH shift
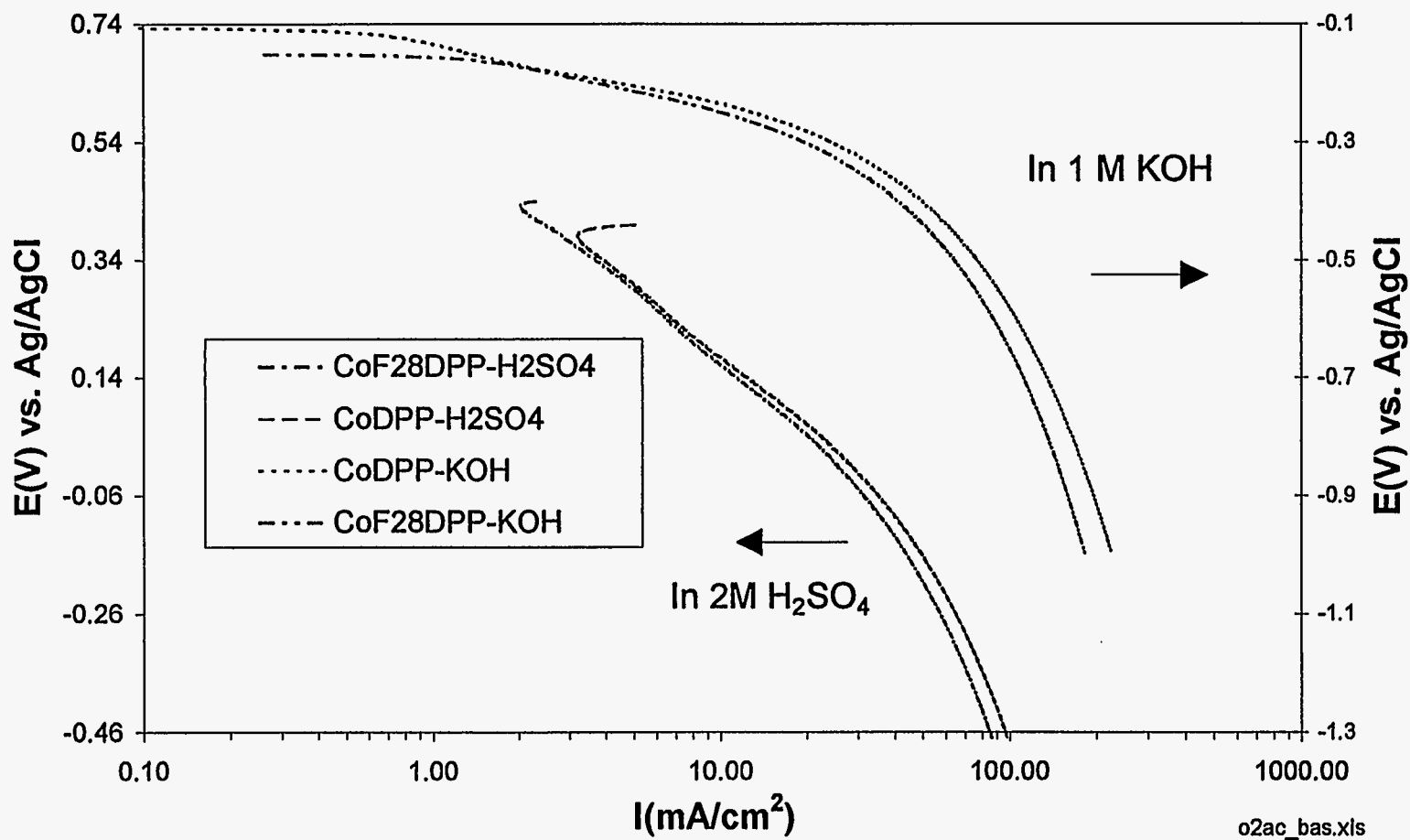

o2ac_bas.xls

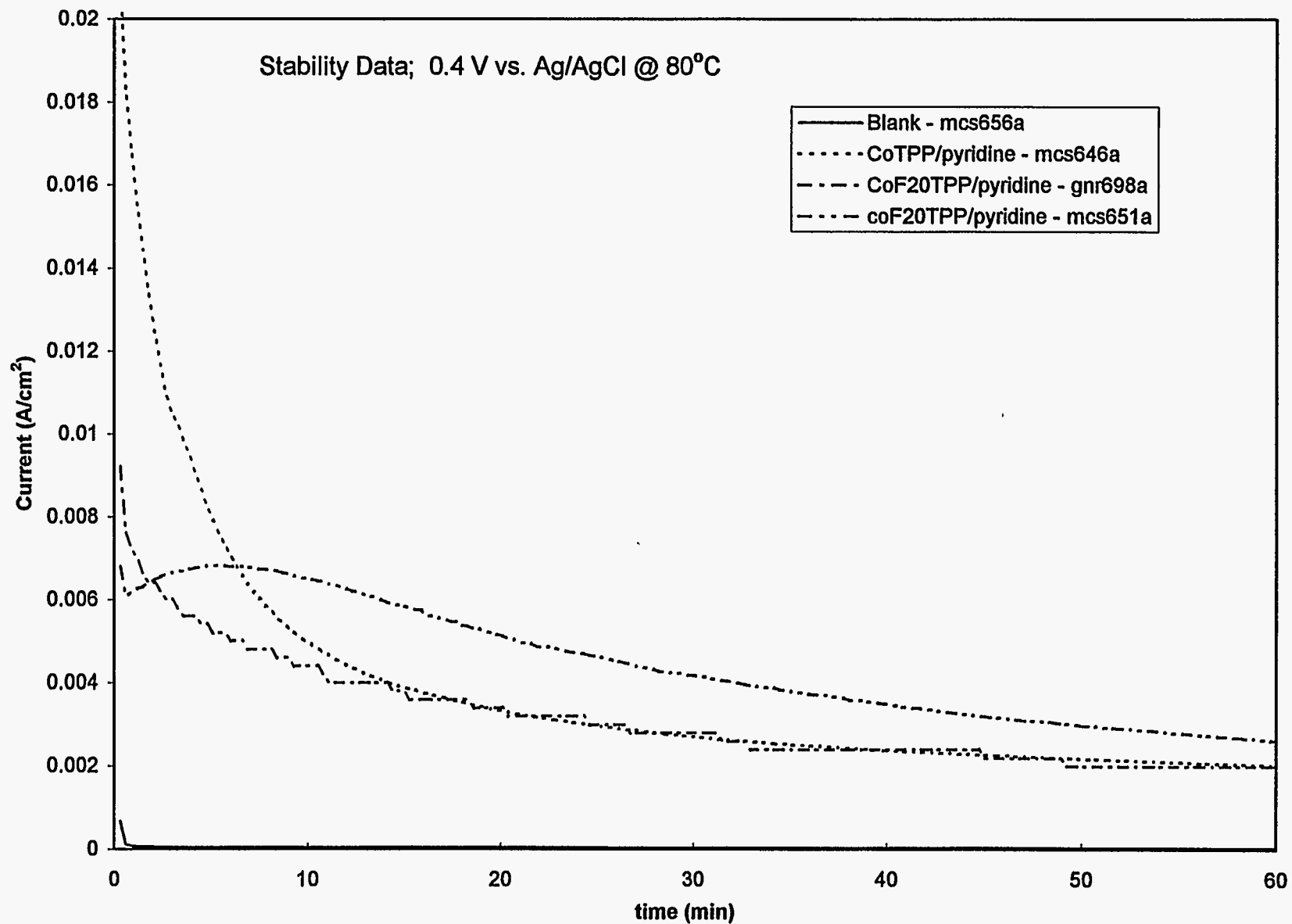*Figure 14 Comparison of performance in acid and base solutions.*

Figure 15 Stability of cobalt tetraphenyl porphyrin electrodes in 2 M sulfuric acid. Oxygen electrode held at 0.4 V. vs Ag/AgCl.

Methanol testing.

Methanol was vaporized into a flowing argon stream and fed into the anode of the Astris cell described above. We were unable to detect electrooxidation of methanol in this apparatus, even using a commercially prepared Pt/Ru electrode. The porphyrins tested included: Fe(III) octaethylporphyrin chloride, Fe(III) tetramethoxyphenylporphyrin chloride, Mg octaethylporphyrin, Mg tetraphenylporphyrin, Zn(II) tetraphenylporphyrin, Zn(II) octaethylporphyirn, and Co tetraphenlyporphyrin. Further work should be performed in this area, since the fact that our Pt/Ru electrodes were ineffective suggests that a better experimental procedure for methanol oxidation is needed.

Spectroscopic Testing

UV-Vis and Raman Spectroscopy:

Resonance Raman spectra were obtained using a partitioned Raman cell and a dual-channel spectrometer. The 413.1-nm line from a krypton ion laser (Coherent, INNOVA 20) and 457.9-nm and 528.7-nm lines from an argon ion laser (Coherent, INNOVA 20) were used for excitation in the Soret- and Q-band regions of the absorption spectrum. The scattered light was collected in the 90° scattering geometry. Polarized spectra were measured by passing the scattered light through a Polaroid sheet oriented parallel or perpendicularly to the polarization direction of the incident beam, followed by a scrambler in front of the spectrometer entrance slit. The spectral slit widths of the spectrometer were in the range of 2 to 6 cm^{-1}. The Raman cell was rotated at 50 Hz to prevent local heating of the sample and to probe alternately the sample and reference solutions.

Detection of Substrate-Catalyst Hydrogen-Bonding Interactions. In an effort to increase the interaction between the catalyst and the substrate oxygen, we began to explore new porphyrins with hydrogen bonding groups, such as the porphyrin shown in Figure 16. H-bonding between substrate molecules and the -NH_2 group of 5-amino-octaethylporphyrin (5-NH_2-OEP) was demonstrated by resonance Raman spectroscopy. The molecular structure of 5-NH_2-OEP is shown in Figure 16 and its resonance Raman spectra in the C-N stretching region of the amino group for various solvent conditions are shown in Figure 17. (Figure 17 also shows the spectrum of NiOEP (unsubstituted) for comparison.) H-bond formation is detected in the resonance Raman spectrum by the upshift in the frequencies and changes in relative intensities of several Raman lines in the region of the C-N stretching vibration of the amino group. No other significant differences are observed in the spectra, indicating negligible effect of H-bonding on the porphyrin macrocycle. Of particular interest are the upshifts in the lines at 1260 and 1382 cm^{-1} and the decrease in the intensity of the latter line. The hydrogen bonding is weak since fairly high concentrations of the H-bonding solvent is required.
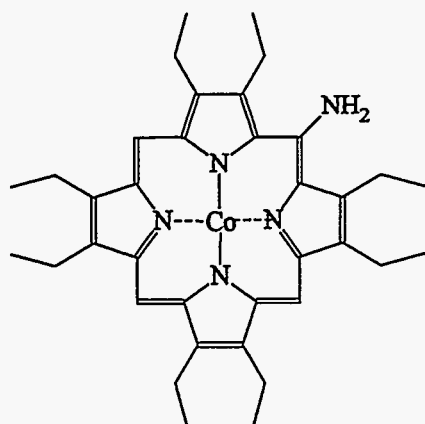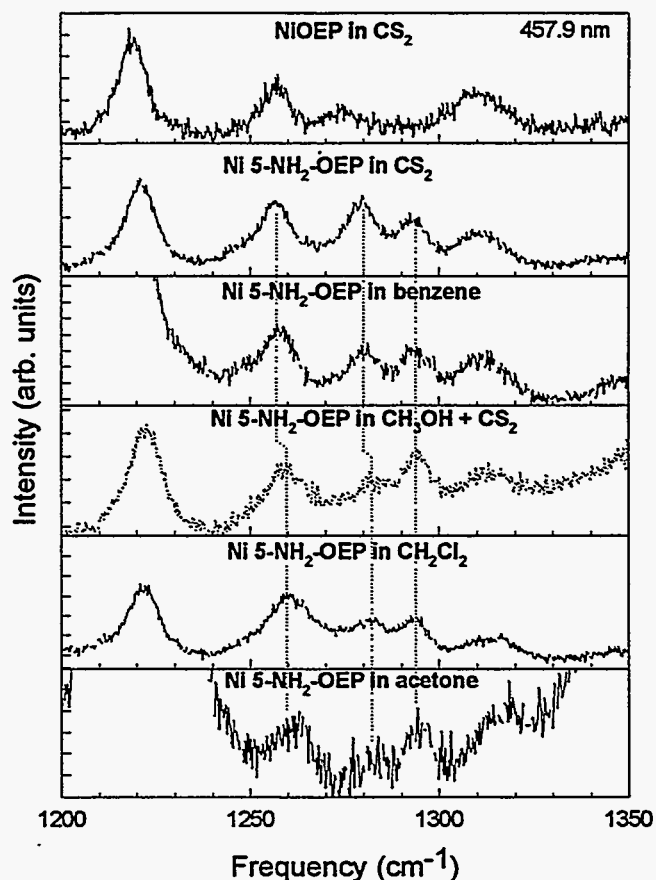
Figure 16. Cobalt 5-amino-octaethyl-porphyrin. The amino group is an H-bond donor and acceptor.

Figure 17 Resonance Raman spectra of nickel(II) 5-NH2-OEP (and NiOEP for comparison) in various solvents. This region of the spectrum contains the C-N stretching vibration which normally occurs in the 1260-1330 cm^{-1} range for primary aromatic amines.

Hydrogen bonding to substrates with H-bond donor groups also may have been detected for 5-monoformyl-octaethylporphyrin (5-CHO-OEP). However, in this case the interpretation is complicated by the presence of two conformers--one for which the formyl group is perpendicular to the plane of the porphyrin and another for which the formyl is parallel to the porphyrin ring and conjugated with the ring. These conformers also differ in the degree of nonplanarity, adding further complexity to any interpretation in terms of H-bonding. The metal derivatives of 5-mono-hydroxyethyl-octaethylporphyrin (5-CH$_2$OH-OEP) have also been synthesized and investigated for H-bonding to donors and acceptors.

Because of these promising results the next step is to synthesize the 5,15-*di*amino-, 5,15-*di*formyl-, and *di*hydroxyethyl-OEP derivatives; molecular modeling suggests much stronger H-bonding to this derivative. At this point, we can say that hydrogen bonding to at least the NH$_2$ group does occur and probably is strong enough to promote substrate binding and conversion, but not so strong as to interfere with catalytic reactions occurring at the metal site. Synthesis of the cobalt derivatives of the 5-amino, 5,10-diamino, and 5,15-diamino derivatives in large enough quantities to test in electrochemical O$_2$-reduction reactions should be a goal of future research in this area. Computer modeling shows that the hydrogen-bonding groups enhance oxygen binding by as much as 16 kcal/mole relative to planar cobalt octaethylporphyrin. (See Molecular Modeling section above.)

Conclusions

Newly designed and synthesized non-planar dodecaphenyl porphyrins appear to have increased catalytic activity in the reduction of oxygen, relative to non-planar porphyrins, as summarized in Figure

13. Initial spectroscopic results with porphyrins having one hydrogen-bonding group suggest that such groups may interact with substrates such as oxygen and that such porphyrins are a promising class of oxygen reduction catalysts. Stability of these new catalysts must be increased to make them viable in the fuel cell environment.

[1] Appleby, A.J.; Foulkes, F.R. Fuel Cell handbook, Krieger Publishing Co., Malabar, Florida, 1993; p. 192.

[2] http://www.er.doe.gov/production/bes/bes.html

[3] R. Jasinski, Nature **201**, 1212 (1964

[4] J. Zagal, M. Paez, A.A. Tanaka, J.R. dos Santos, Jr., *J. Electroanal. Chem.* **1992**, *339*, 13

[5] D. F. Rohrbach, E. Deutsch, W. R. Heineman, R. F. Pasternack, *Inorg. Chem.* **1977**, *16*, 2650

[6] J.P. Collman, M. Marrocco, P. Denisevich, C. Koval, F.C. Anson, *J. Electroanal. Chem.* **1979**, *101*, 117; J.P. Collman, P. Denisevich, Y. Kohai, M. Marrocco, C. Koval, F.C. Anson, *J. Am. Chem. Soc.* **1980**, *102*, 6027

[7] C. Shi, F. C. Anson, *Inorg. Chem.* **1992**, *31*, 5078.

[8] Electrosynthesis Co., Lancaster, NY

[9] M. Ladouceur, G. Lalande, D. Guay, J.P. Dodelet, L. Dignard-Bailey, M. L. Trudeau, R. Schulz, *J. Electrochem. Soc.* **1993**, *140*, 1974; M. C. Martins Alves, J. P. Dodelet, D. Guay, M. Ladouceur, G. Tourillon, *J. Phys. Chem.* **1992**, *96*, 10898

[10] A. Widelov, R. Larsson, *Electrochim. Acta* **1992**, *35*, 187

DISTRIBUTION:

1	MS	0710	G.N. Ryba, 6210
1		0710	J.A. Shelnutt, 6210
1		0342	K. R. Zavadil, 1823
1		0614	N. Doddapaneni, 1523
1		0188	LDRD Office, 4523
1		9018	Central Technical Files, 8940-2
5		0899	Technical Library, 4414
2		0619	Review & Approval Desk, 12690
			For DOE/OSTI